Transactions on Modelling and Simulation vol 18, © 1997 WIT Press, www.witpress.com, ISSN 1743-355X

Non-conforming BEM discretisation in frictional elastoplastic contact problems

D. Martín and M. H. Aliabadi
Wessex Institute of Technology, Ashurst Lodge, Ashurst, Southampton SO40 7AA, UK

Abstract - *In this paper, elastoplastic contact problems with friction are solved by BEM, using non conforming discretisation. The contact conditions are directly enforced by relating tractions and displacements at every node of the contact zone with a point on the opposite surface. An initial strain BEM formulation is used to study the elastoplastic problem. The material is assumed to obey the Von Mises yield criterion with its associated flow rule. A numerical application is presented, and the results are compared to those obtained by the use of conforming discretisation.*

Introduction

The BEM is a powerful and efficient numerical technique for solving contact problems, as contact is inherent to the boundaries of the bodies involved. The application of BEM to a range of elastostatic, frictional problems is now well established, see for example Andersson [1], Karami and Fenner [2], París and Garrido [3] and Man, Aliabadi and Rooke [4]. These formulations use a direct contraint technique, whereby the solution is obtained explicitly from equilibrium and compabitility conditions.

The use of conforming discretisations is a common feature of the research works cited above. The contact areas are modelled in such a way that for every node on one body, there must be a matching node on the other. These two nodes form a node-pair, which allows the enforcement of the appropriate contact conditions, by relating the corresponding unknowns in the system of equations.

BEM formulations for contact problems are currently being revised in order to remove the need of conforming discretisations, which are increasingly regarded as an unnecessary limitation. [5], [6], [7]. The use of non-conforming discretisations allows the solution of a wider range of problems, like those involving large relative displacements, and simplifies the modelling and data preparation, particularly in the case of non-conforming problems, in which the surfaces in contact have different shapes before the application of the loads.

The need to include elastoplasticity is important for some type of problems, and has received attention from researchers using BEM [8-12], all of which are restricted to the use of conforming discretisations. The use of non-conforming discretisation to solve frictionless, elastoplastic contact problems is reported in [13].

The work presented in this paper describes the solution of elastoplastic contact problems without the use of conforming discretisations. To this end, the unknowns of a given node within the contact zone of one of the bodies are related to those of an opposite point on the boundary of the other body, which in turn are expressed in terms of the nodal unknowns by means of the shape functions. The contact areas are modelled using standard quadratic elements.

The initial strain approach for the elastoplastic BEM formulation [14] is employed here. The material is assumed to obey the Von Mises yield criterion with its associated flow

rule [15]. The model can handle either perfectly plastic or work hardening materials.

BE Formulation for Elastoplastic Problems

In order to solve an elastoplastic problem by means of the BEM the inelastic strains are considered as initial strains [14]. With this in mind, and considering a homogeneous body of domain Ω, enclosed by a boundary Γ, the following integral equation can be written for the displacement rate $\dot{u}_j$ at a point $\mathbf{z}' \in \Gamma$:

$$c_{ij}(\mathbf{z}')\,\dot{u}_j(\mathbf{z}') + \oint_\Gamma T_{ij}(\mathbf{z}',\mathbf{x}')\,\dot{u}_j(\mathbf{x}')\,d\Gamma(\mathbf{x}') = \int_\Gamma U_{ij}(\mathbf{z}',\mathbf{x}')\,\dot{t}_j(\mathbf{x}')\,d\Gamma(\mathbf{x}') + \\ + \int_\Omega \sigma^*_{ijk}(\mathbf{z}',\mathbf{x})\;\dot{\varepsilon}^p_{jk}(\mathbf{x})\;d\Omega(\mathbf{x}), \tag{1}$$

where $\mathbf{x}'$ refers to a point on the boundary Γ and $\mathbf{x}$ to a point in the domain Ω; $\dot{u}_j$, $\dot{t}_j$ are the displacement and traction rates respectively; $\dot{\varepsilon}^p_{jk}$ is the plastic strain rate; T_{ij}, U_{ij} and σ^*_{ijk} are the fundamental solutions of elasticity. The symbol $\oint$ indicates a Cauchy principal value integral and c_{ij} is a constant that depends on the geometry of the boundary at $\mathbf{z}'$. Although no time-dependent effects are studied here, the rate notation is used to indicate that the magnitudes involved depend on the loading history.
The stress integral equation valid for the stress rates at an internal point $\mathbf{z}$ can be obtained by differentiating (1) with respect to the coordinates of $\mathbf{z}$ and applying the generalised Hooke's law to the elastic part of the total strain rate tensor, to give:

$$\dot{\sigma}_{ij}(\mathbf{z}) = \int_\Gamma U_{ijk}(\mathbf{z},\mathbf{x}')\dot{t}_k(\mathbf{x}')d\Gamma(\mathbf{x}') - \int_\Gamma T_{ijk}(\mathbf{z},\mathbf{x}')\dot{u}_k(\mathbf{x}')d\Gamma(\mathbf{x}') \\ + \oint_\Omega \Sigma^*_{ijkl}(\mathbf{z},\mathbf{x})\dot{\varepsilon}^p_{kl}(\mathbf{x})d\Omega(\mathbf{x}) + f_{ij}(\dot{\varepsilon}^p_{kl}(\mathbf{z})), \tag{2}$$

where U_{ijk}, T_{ijk} and Σ^*_{ijkl} are the fundamental solutions, and the free term f_{ij} results from the differentiation of the domain integral that appears in equation (1).
After discretising the boundary and those areas of the domain where yielding is expected to occur, and after a collocation procedure, (1) and (2) can be written in matrix form as:

$$\mathbf{H}\dot{\mathbf{u}} = \mathbf{G}\dot{\mathbf{t}} + \mathbf{D}\dot{\varepsilon}^{\mathbf{P}} \tag{3}$$

and

$$\dot{\sigma} = \mathbf{G}'\dot{\mathbf{t}} - \mathbf{H}'\dot{\mathbf{u}} + (\mathbf{D}' + \mathbf{C}')\dot{\varepsilon}^{\mathbf{P}}. \tag{4}$$

The vectors $\dot{\mathbf{u}}$ and $\dot{\mathbf{t}}$ contain the values of displacement and traction rates at all boundary nodes. Vector $\dot{\varepsilon}^{\mathbf{P}}$ contains the plastic strain rates $\{\dot{\varepsilon}^{\mathbf{P}}_1, \dot{\varepsilon}^{\mathbf{P}}_2, \dot{\varepsilon}^{\mathbf{P}}_{12}\}$ at both internal and boundary control points. Since equation (2) is only valid for internal points, the stress rates at boundary points must be computed from different expressions. The resulting coefficients can be assembled into equation (4) and thus, the stress rates can be calculated in a unified way. Equation (3) can be rearranged according to the boundary conditions, which gives the final system of equations:

$$\mathbf{A}\dot{\mathbf{y}} = \dot{\mathbf{f}} + \mathbf{D}\dot{\varepsilon}^{\mathbf{P}}, \tag{5}$$

where $\dot{\mathbf{y}}$ is the vector of the unknowns, and $\dot{\mathbf{f}}$ is the elastic part of the right hand side vector, which contains the contribution of the known boundary conditions.
Similarly, equation (4) can also be rearranged to give:

$$\dot{\sigma} = -\mathbf{A}'\dot{\mathbf{y}} + \dot{\mathbf{f}}' + \mathbf{D}^*\dot{\varepsilon}^{\mathbf{P}}, \tag{6}$$

where $\mathbf{D}^*=(\mathbf{D}'+\mathbf{C}')$, $\mathbf{A}'$ contains the corresponding columns of $\mathbf{H}'$ and $\mathbf{G}'$; and $\dot{\mathbf{f}}'$ includes the contribution of the prescribed values.
A yield criterion indicates the stress level at which plastic flow commences. In particular, the Von Mises yield criterion, suitable for metals is used here. For a multiaxial stress state, an equivalent stress is defined as:

$$\sigma_{eq} = \sqrt{3J_2} \tag{7}$$

where J_2 is the second invariant of the deviatoric stress tensor, S_{ij}, and yielding occurs whenever the equivalent stress reaches the value of the uniaxial yield stress, σ_0:

$$\sqrt{3J_2} - \sigma_0 = 0 \tag{8}$$

Therefore the load at first yield can be calculated from the elastic solution of equations (5) and (6) (with $\dot{\varepsilon}^p = 0$). The most highly stressed boundary node or internal point must be taken, and its equivalent stress σ_{eq}^{max} reduced to the uniaxial yield stress of the material, σ_0.
The remaining load has to be applied incrementally. Equations (5) and (6) can be rewritten as:

$$\mathbf{A}\mathbf{y} = \mathbf{f} + \mathbf{D}(\varepsilon^{\mathbf{P}} + \mathbf{\Delta}\varepsilon^{\mathbf{P}}) \tag{9}$$

and

$$\sigma = -\mathbf{A}'\mathbf{y} + \mathbf{f}' + \mathbf{D}^*(\varepsilon^{\mathbf{P}} + \mathbf{\Delta}\varepsilon^{\mathbf{P}}), \tag{10}$$

where $\varepsilon^{\mathbf{P}}$ represents the accumulated plastic strains up to, but not including the corresponding to the current load increment $\mathbf{\Delta}\varepsilon^{\mathbf{P}}$, which are to be determined iteratively, as follows:

(a) Arbitrary initial guess for $\mathbf{\Delta}\varepsilon^{\mathbf{P}}$.

(b) Compute $\mathbf{y}$, σ. (Eqs. (9) and (10)).

(c) Use stress-strain relationship for post yield behaviour to obtain a new estimate for $\mathbf{\Delta}\varepsilon^{\mathbf{P}}$.

(d) Go to **(b)** until convergence within prescribed tolerance is achieved.

Once convergence is obtained at all control points $\mathbf{\Delta}\varepsilon^{\mathbf{P}}$ is added to $\varepsilon^{\mathbf{P}}$, and its value is also used as an initial guess for the next load increment.

Contact Problems

Solving a contact problem requires the determination of tractions and displacements that arise within the contact areas, which are not prescribed as boundary conditions. The direct constraint technique consists of writing compatibility and equilibrium conditions as additional equations to couple the unknowns of the nodes brought into contact. In order to solve the elastoplastic contact problem, it is necessary to apply equation (9) to all the bodies involved. For example, for two bodies in contact, and using a superscript for each of them:

$$\begin{array}{|c|c|}\hline \mathbf{A^1} & \mathbf{0} \\ \hline \mathbf{0} & \mathbf{A^2} \\ \hline \multicolumn{2}{|c|}{\textbf{Contact Conditions}} \\ \hline \end{array} \begin{array}{|c|}\hline \mathbf{y^1} \\ \hline \mathbf{y^2} \\ \hline \end{array} = \begin{array}{|c|}\hline \mathbf{f^1} \\ \hline \mathbf{f^2} \\ \hline \mathbf{0} \\ \hline \end{array} + \begin{array}{|c|c|}\hline \mathbf{D^1} & \mathbf{0} \\ \hline \mathbf{0} & \mathbf{D^2} \\ \hline \mathbf{0} & \mathbf{0} \\ \hline \end{array} \begin{array}{|c|}\hline \varepsilon^{p^1} + \Delta\varepsilon^{p^1} \\ \hline \varepsilon^{p^2} + \Delta\varepsilon^{p^2} \\ \hline \end{array} \tag{11}$$

In the presence of friction, the **Contact Conditions** in equation (11) depend upon the contact modes, *i.e.* stick or slip, as shown in table (1).

Slip	**Stick**
$t_t^a + t_t^b = 0$	$t_t^a + t_t^b = 0$
$t_n^a + t_n^b = 0$	$t_n^a + t_n^b = 0$
$t_t^a \pm \mu t_n^a = 0$	$u_t^a - u_t^b = 0$
$u_n^a - u_n^b = 0$	$u_n^a - u_n^b = 0$

Table 1: Modes of contact

The contact modes at each control pair are not known in advance, and therefore they must be determined iteratively. The contact modes are first set arbitrarily to slip, and after the solution, they are checked against inconsistencies. The tangential tractions must oppose the relative tangential displacemente at a *slip* control pair. A *stick* control pair must have a tangential traction which is lower than its maximum value, *i.e.* the normal traction times the friction coefficient. If there exists any violation to these conditions, the contact modes are changed, and the problem is solved again. The solution of equation (11) requires the computation of the inverse of matrix $\mathbf{A}$. Inverting it every time the contact conditions change would be a very expensive task. Special schemes, such as the Sherman-Morrison-Woodbury formula [16] can be used to obtain the inverse of a matrix, after small changes happen to the original one.
In order to compute the internal stresses equation (10) is written for each body separately:

$$\sigma^1 = -\mathbf{A'^1 y^1} + \mathbf{f'^1} + \mathbf{D^{*1}}(\varepsilon^{\mathbf{p1}} + \mathbf{\Delta}\varepsilon^{\mathbf{p1}}) \tag{12}$$

$$\sigma^2 = -\mathbf{A'^2 y^2} + \mathbf{f'^2} + \mathbf{D^{*2}}(\varepsilon^{\mathbf{p2}} + \mathbf{\Delta}\varepsilon^{\mathbf{p2}}). \tag{13}$$

Equations (11), (12) and (13) are then solved for the current load step, where the iterative procedure to determine $\mathbf{\Delta}\varepsilon^{\mathbf{p}}$ must be carried out.

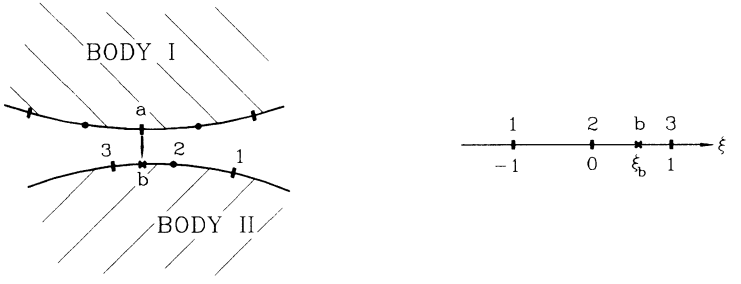

a) GEOMETRY b) INTRINSIC COORDINATES

Figure 1: Node a and Point b

Non-Conforming Discretisation

Figure (1) shows the general case of non-conforming discretisation, in which a node a is brought into contact with a point b, which does not belong to the original boundary discretisation. Its position within the element is determined by the intrinsic coordinate, ξ_b, subject to the condition $\xi_b \neq \pm 1$, $\xi_b \neq 0$.

In order to avoid considering u_t^b, u_n^b, t_t^b and t_n^b as additional unknowns they can be expressed in terms of the variables of nodes 1, 2 and 3 by using the shape functions, as follows:

$$\begin{cases} u_t^b = \sum_{k=1}^{3} u_t^k N^k(\xi_b) \\ u_n^b = \sum_{k=1}^{3} u_n^k N^k(\xi_b) \\ t_t^b = \sum_{k=1}^{3} t_t^k N^k(\xi_b) \\ t_n^b = \sum_{k=1}^{3} t_n^k N^k(\xi_b) \end{cases} \tag{14}$$

For a node a comprised in the original discretisation two equations must be written in order to balance the number of unknowns, in addition to the displacement equations (1). Therefore, writing conditions shown in table (1) into the system of equations would result in an overdetermination. Only two of them must be chosen and it is inevitable that those conditions not explicitly enforced will result violated (albeit by a small margin) in the final solution.

The best results are obtained when a balanced combination of compatibility and equilibrium conditions is used. More specifically, equilibrium conditions are enforced at every node of body I, and compatibility conditions are enforced at every node of body II.

According to the contact modes, and making use of equations (14), the equilibrium conditions for a node a of body I are:

a) Slip

$$t_t^a = \pm \mu t_n^a$$

$$t_n^a = -\sum_{k=1}^{3} t_n^k N^k(\xi_b) \tag{15}$$

b) Stick

$$t_t^a = -\sum_{k=1}^{3} t_t^k N^k(\xi_b)$$

$$t_n^a = -\sum_{k=1}^{3} t_n^k N^k(\xi_b) \tag{16}$$

while for nodes of body II (notation a, b is maintained for convenience) the compatibility conditions are:
a) Slip

$$t_t^a = \pm \mu t_n^a$$

$$u_n^a = \sum_{k=1}^{3} u_n^k N^k(\xi_b) \tag{17}$$

b) Stick

$$u_t^a = \sum_{k=1}^{3} u_t^k N^k(\xi_b)$$

$$u_n^a = \sum_{k=1}^{3} u_n^k N^k(\xi_b) \tag{18}$$

Equations (15) to (18) can be expressed in matrix form, and assembled in equation (11) as **Contact Conditions**.

Numerical Application

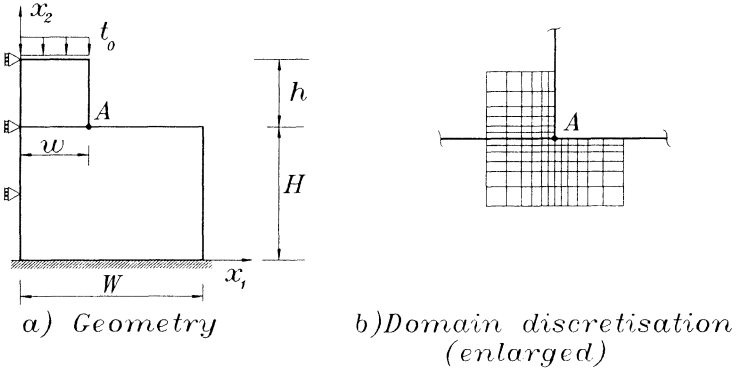

Figure 2: Flat punch

A conforming contact problem is analysed, where the contact area does not depend on the external load. It presents, however, a singularity at point A (see figure (2a)), and in the presence of friction the partition between the *stick* and *slip* zones must be determined iteratively.

A flat punch of semi-width w and height h lies on a foundation of semi-width W and height H, respectively. The ratios between them are assumed to be $h/w = 2$, $H/W = 1$ and $w/W = 1/4$, where $W = 160$ mm. The domain discretisation in the neighbourhood of the corner of the punch is shown in figure (2b). A uniform compressive load per unit thickness, t_0, is applied on the upper face of the punch.

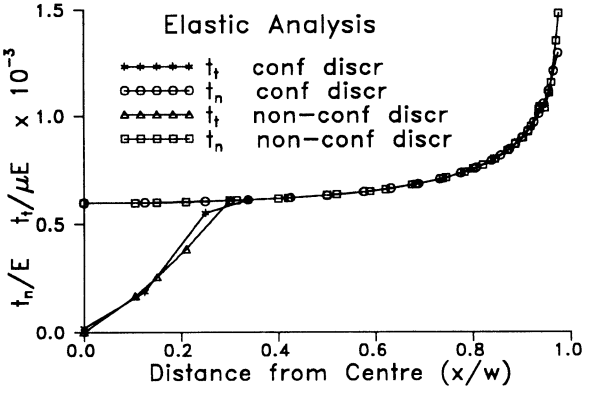

Figure 3: Elastic Contact Tractions

The punch and the foundation are assumed to have the following material properties: elastic modulus $E = 210$ GPa; Poisson's ratio $\nu = 0.3$; yield stress $\sigma_Y = 196$ MPa; plastic modulus $H' = 900MPa$ (work hardening material). The friction coefficient is taken as $\mu = 0.15$. The problem is solved under plane strain condition.

This example is discretised using 75 quadratic boundary elements and 63 internal cells. The contact area of the foundation is discretised using 8 elements, whereas a finer mesh of 11 elements is used to discretise the contact area of the punch.

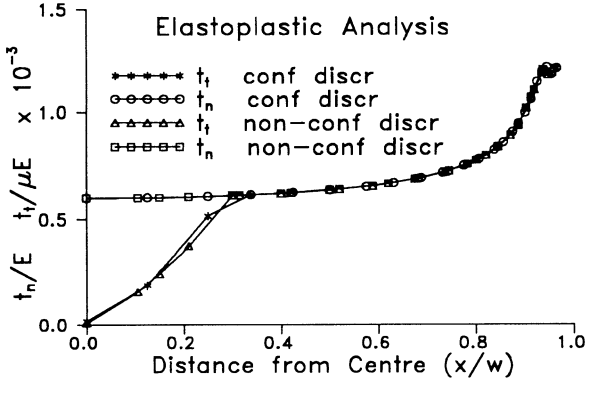

Figure 4: Elastoplastic Contact Tractions

Figure (3) shows the elastic values of the normal and tangential contact tractions obtained for a load $t_o = 150$ MN/m. The partition between *stick* and *slip* zones is situated at $x/w = 0.33$, although it is not well defined for the conforming case, as the mesh employed is not refined enough. Nevertheless, the results for both cases compare generally well.

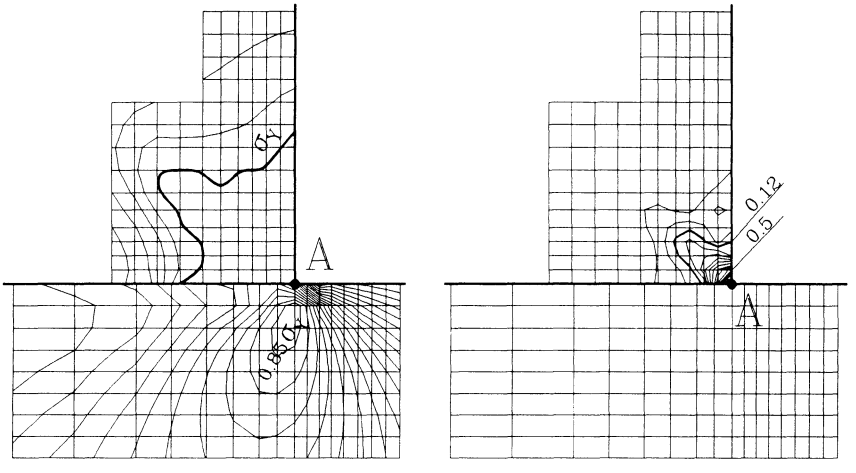

Figure 5: Plastic Stresses and Strains

In figure(4) the values of the normal and tangential contact tractions obtained for the elastoplastic case are shown. The first node to become plastic is the lower right corner of the punch, point A. The value of the load for which this happens, or load at first yield, is $t_{oY} = 44.6$ MN/m. The remaining load is applied in 11 steps, until the final value of $t_o = 150$ MN/m is reached.

In this case, the formation of a plastic zone limits the maximum value of the normal traction and the position in which it occurs is shifted from point A towards the interior of the contact area. The partition between the *stick* and *slip* zone does not change significantly from the elastic analysis, which is to be expected, since the plastic zone is situated at a certain distance away.

Figure (5) shows the distribution of Von Mises stresses and equivalent plastic strains. The plastic zone develops only within the punch, and has a roughly rectangular shape. The foundation remains in elastic regime throughout the loading process. The maximum stresses occur inside the body. A high stress gradient from the maximum value under the corner of the punch to nearly zero on the free surface is observed.

Conclusions

BEM contact formulations requiring the use of conforming discretisations are currently being superseded by more advanced approaches which allow node-on-element contact schemes. In this paper, elastoplastic contact problems with friction are solved using non-conforming discretisations. The contact conditions are directly enforced by relating tractions and displacements at every node of the contact zone with points on the opposite surface by means of the shape functions. Frictional phenomena are considered by employing Coulomb's friction law. The contact modes are determined iteratively, as these are not known in advance.

A BEM initial strain approach is used to model the elastoplastic response of the material. The Von Mises yield criterion with its associated flow rule is adopted. The approach is capable of handling elastic-perfectly plastic as well as work hardening constitutive relationships.

The obtained results, in particular the sensitive tangential tractions, compare favourably to those obtained using conforming discretisations.

References

1. T. Andersson, *Boundary Elements in two-dimensional Contact and Friction. Dissertations. No. 85*, Linköping University, 1982.
2. G. Karami, R.T. Fenner, A Two-Dimensional BEM Method for Thermo-Elastic Body Forces Contact Problems, in *Boundary Elements IX, Vol 2: Stress Analysis Applications*, C.A. Brebbia, W.L. Wendland and G. Kuhn, Eds., Computational Mechanics Publications, Southampton, Springer-Verlag, Berlin, pp. 417-437, 1987.
3. F. París, J.A. Garrido, On the Use of Discontinuous Elements in 2D Contact Problems. *Boundary Elements VII*, pp 13-27 to 13-39. Computational Mechanics Publications, Southampton, 1985.
4. K.W. Man, M.H. Aliabadi, D.P. Rooke, Analysis of Contact Friction using the Boundary Element Method, in *Computational Methods in Contact Mechanics*, M.H. Aliabadi and C.A. Brebbia, Eds., Computational Mechanics Publications, Southampton, Elsevier Applied Science, London, pp. 1-60, 1993.
5. A. Blázquez, F. París, J. Cañas, J.A. Garrido, An algorithm for frictionless contact problems with non-conforming discretizations using BEM, in *Boundary Elements XIV*, C.A. Brebbia, J. Domínguez and F. París, Eds., Computational Mechanics Publications, Southampton, pp. 409-420, 1992.
6. O.A. Olukoko, R.T. Fenner, A new boundary element approach for contact problems with friction. *Int. J. Numer. Meth. Engng.*, Vol. 36, pp. 2625-2642, 1993.
7. A. Huesmann, G. Kuhn, Non-conform discretisation of the contact region applied to two-dimensional Boundary Element Method, in *Boundary Elements XVI*, C.A. Brebbia, Ed., Computational Mechanics Publications, Southampton, pp.353-360, 1994.
8. M. Alcantud, M. Doblaré, L. Gracia, J. Domínguez, Analysis of the Contact Problems Between Elastoplastic 2-D Bodies by Means of the BEM, in *Boundary Elements in Mechanical and Electrical Engineering*, C.A. Brebbia and A. Chaudouet-Miranda, Eds., Computational Mechanics Publications, Southampton, Springer-Verlag, Berlin, pp. 15-30, 1990.
9. G. Karami, Boundary Element Analysis of Elasto-plastic Contact Problems, *Computers & Structures*, 41, pp. 927-935, 1991.
10. V.M.A. Leitão, M.H. Aliabadi, D.P. Rooke, Elastoplastic Dual Boundary Elements: Application to Crack Problems, in *Boundary Element Technology IX*, C.A. Brebbia, A.J Kassab, Eds., Computational Mechanics Publications, Southampton, pp. 213-225, 1994.
11. D. Martín, M.H. Aliabadi, V.M.A. Leitão, Application of BEM to Elastoplastic Contact Problems, in *Boundary Elements XVI*, C.A. Brebbia, Ed., Computational Mechanics Publications, Southampton, pp.337-344, 1994.
12. D. Martín, M.H. Aliabadi, Application of BEM to Non-conforming Elastoplastic Contact Problems, in *Contact Mechanics II, Computational Techniques*, M.H. Aliabadi, C. Alessandri, Eds., Computational Mechanics Publications, Southampton, pp. 313-321, 1995.
13. D. Martín, M.H. Aliabadi, Non-conforming BEM discretisation in elastoplastic contact problems, in *Computational Methods in Contact Mechanics III*, M.H. Aliabadi and A. Samartin, Eds., Computational Mechanics Publications, Southampton, pp. 71-79, 1997.
14. C.A. Brebbia, J.C.F. Telles, L.C. Wrobel, *Boundary Element Techniques*, Springer-Verlag, Berlin, 1984.
15. A. Mendelson, *Plasticity: Theory and Application*, Macmillan, New York, 1968.
16. W.H. Press, S.A. Teukolsky, W.T. Vetterling, B.P. Flannery, *Numerical Recipes in FORTRAN*, Cambridge University Press, 1992.